Ageostrophic effects in rotating stratified flow

By HERBERT E. HUPPERT

Department of Applied Mathematics and Theoretical Physics, University of Cambridge

AND MELVIN E. STERN

Graduate School of Oceanography, University of Rhode Island, Kingston, Rhode Island 02881

We consider the low Rossby number (R) flow of a stratified fluid in a long rotating channel, for which the bottom elevation varies in the downstream direction. The quasi-geostrophic response is shown to be singular at the side walls of the channel, and thus an ageostrophic analysis is necessary even for vanishingly small R. Part of the ageostrophic steady-state response is a modified quasi-geostrophic perturbation trapped near the bottom. A second component which is present even as R approaches zero is an internal Kelvin wave whose vertical wavelength adjusts so that the wave remains stationary with respect to the channel bottom and which propagates energy and momentum to infinite heights in an unbounded channel. The case of a bounded layer of fluid is also considered, and the resonance conditions are given. We also calculate the flow field when the bottom elevation varies in the cross-stream direction. We conclude that stagnation or flow reversal can be caused either by the modified quasi-geostrophic component or by the Kelvin wave and estimate the critical condition by an extrapolation of the perturbation velocity computed from linear theory.

1. Introduction

The major part of the energy in geophysical flows is in the large-scale motions, a fact which is often explicitly taken into account by considering a quasi-geostrophic development of the equations of motion. In such a development the velocities which appear in the equation for the time rate of change of the vertical vorticity are determined from the zeroth-order balance between the Coriolis force and the pressure gradient. It is known, however, that this procedure has the effect of filtering out the inertia–gravity waves which would otherwise be present in a shallow-water, or hydrostatic formulation. If there exist systematic couplings between geostrophic and inertial scales over long periods of time, then such interactions will be excluded from a quasi-geostrophic analysis. For example, recent observations (Parker 1971; Richardson, Strong & Knauss 1973) have shown that the geostrophic eddies which are shed from the Gulf Stream take a number of years to decay, and the mechanism by which energy is lost is unknown. This mechanism is of considerable importance in developing an understanding of the energy balance of the fluctuations in the large-scale circulation. In addition, we note that there are many unresolved questions regarding large amplitude inertial wave packets (Webster 1968). A question which hence arises is whether

there can be significant spectral coupling between these two forms of motion, whereby the energy that is lost from the geostrophic eddies reappears as a source for inertial oscillations.

Although we do not here address ourselves directly to the geophysical question raised above, we believe that the theoretical and experimental investigation of ageostrophic effects in simple systems such as that considered below illuminates some of the possible interaction processes. The spectral coupling in our example is provided by the flow of a stratified fluid over variable bottom topography between vertical walls in a uniformly rotating system. As such it represents an extension of the many investigations of stratified flow over an obstacle, as documented, for example, by Miles (1969). The novel addition of our analysis is the inclusion of vertical walls, in consequence of which the response contains a significant internal Kelvin wave and other ageostrophic effects even as the Rossby number approaches zero.

In order to explain some of the features which occur in a stratified fluid we first consider, in §2, the flow of a homogeneous fluid over a smoothly varying step between two vertical walls (figure 1). The nonlinear potential vorticity equation can be integrated exactly in this situation to determine the downstream velocity in terms of the uniform flow. Given the geometry and rotation rate, for sufficiently large upstream velocities, the flow everywhere has a positive downstream component. A critical upstream velocity exists, however, below which the flow in part of the channel is blocked in the sense that no streamline originating upstream enters this blocked region. Part of the analysis presented below is aimed at investigating the corresponding effect of streamline stagnation for a stratified fluid.

The analysis is developed for the stratified flow over a fixed bottom of small slope in an infinitely long channel (figure 2), though a laboratory experiment might be more conveniently performed by towing an obstacle over the bottom through an otherwise quiescent fluid. In addition, our infinitely long channel might be replaced in the laboratory by an annulus of width small compared with its radius. Either way, a quasi-geostrophic analysis for sufficiently long waves or sufficiently small relative speeds V yields a simple geostrophic response with the disturbance trapped near the bottom by the stratification.

This is not the complete response, however. No matter how small the Rossby number is there will always be an internal Kelvin wave generated that is stationary with respect to the obstacle and whose vertical wavelength is thus determined by the flow speed and the static stability. The Kelvin wave transfers energy and momentum to infinite heights in an unbounded fluid, while in a bounded fluid it can cause resonant amplification if V is small or a hydraulic jump if V exceeds the maximum horizontal velocity of a free Kelvin wave. In the simplest geometry, for which there is no variation in the bottom topography across the channel, the quasi-geostrophic analysis is singular and leads to infinite velocities in the channel corners. An ageostrophic analysis eliminates this difficulty and indicates that the velocities are everywhere bounded with a magnitude which varies logarithmically with Rossby number for small Rossby numbers. This ageostrophic effect is weakened if the bottom topography varies smoothly across the channel in such a

way that the height of the bottom vanishes at the side walls. In this case, the quasi-geostrophic analysis predicts velocities which are everywhere bounded.

The linearized analysis developed may be extended to calculate the critical value of the inverse Froude number, based on the Brunt–Väisälä frequency and the maximum obstacle height, in excess of which blocking occurs. For a constant cross-channel bottom topography, the critical value can be determined only by an ageostrophic analysis, no matter how small the Rossby number. This is because the quasi-geostrophic calculation leads to the infinite velocities mentioned above and indicates that the flow is blocked for all inverse Froude numbers. For a bottom topography which varies across the channel, the calculation, to which the ageostrophic effects also make an important contribution, does not include the nonlinear effects associated with the flow of fluid around rather than over the topography and so the critical value obtained will not be as accurate. Nevertheless, it is interesting to determine for a number of different obstacles even approximate values of the inverse Froude number above which blocked regions exist.

Such blocked regions, or Taylor columns, over isolated obstacles have been recently investigated by Hogg (1973) and Huppert (1974) using quasi-geostrophic analysis for a horizontally infinite, stratified fluid. Taylor columns exist in infinite media because when an obstacle is accelerated from rest to a constant speed, say V, some of the disturbances generated by the obstacle have vanishing group velocity and hence remain near the obstacle, since they cannot radiate their energy. These disturbances will be altered by the presence of side walls because part of their energy can now be radiated by the Kelvin wave. While the investigation of such a situation is beyond our analysis, we wish to point out the importance of side walls to the Taylor-column problem and suggest that their influence be investigated further.

After discussing the flow of a homogeneous fluid in a rotating channel in §2, we develop the equations describing the flow of a stratified fluid over a varying bottom topography in a rotating channel of infinite height in §3. We first consider the flow over a bottom which varies sinusoidally in the downstream direction, making use of the simplification that the downstream wavelength is large compared with the channel width, the consequences of which we examine in appendix A. The solution for the flow over an arbitrary bottom is then obtained using Fourier superposition. We discuss the character of this solution and calculate the critical inverse Froude number for a number of different bottom topographies in §4. In §5, we briefly examine the flow in a channel with only one wall. A summary of our more important results is presented in the concluding section.

2. Stagnation of a homogeneous flow

We investigate first some elementary properties of the flow of a homogeneous rotating fluid and then use these ideas in developing an understanding of the stratified flow regime. Consider the system shown in elevation in figure 1. The channel, which is doubly infinite in the y direction, consists of two vertical walls at $x = 0$ and $x = L$, a horizontal upper lid at $z = H$ and a gradually sloping
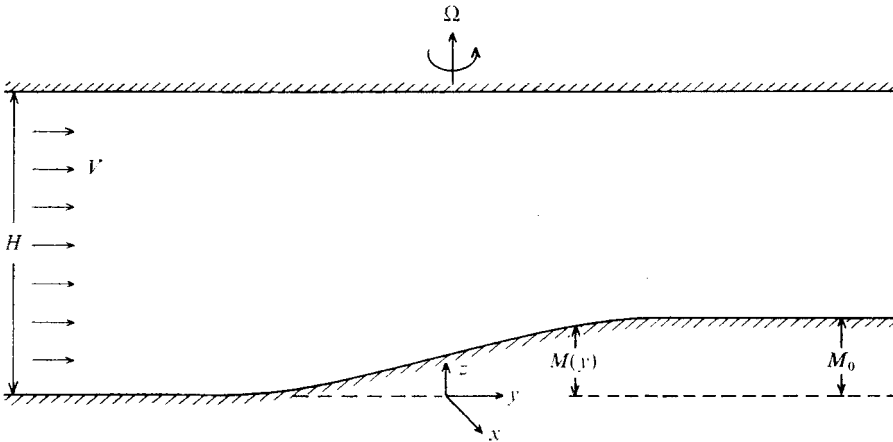
FIGURE 1. An elevation of the channel, bounded by vertical walls at
$x = 0, L$, which is considered in §2.

bottom at $z = M(y)$, with $M(-\infty) = 0$ and $M(\infty) = M_0$. The channel rotates
about the vertical axis with angular velocity $\Omega \equiv \frac{1}{2}f$.

The dynamics for the inviscid motion of columns of fluid in a shallow layer are
described by the conservation of potential vorticity equation

$$\frac{D}{Dt}\left(\frac{f+\xi}{H-M}\right) = 0, \tag{2.1}$$

where ξ is the relative vorticity. If the flow far upstream is uniform the potential
vorticity has the uniform value f/H. It then follows from (2.1) that $(f+\xi)/(H-M)$
is constant everywhere. The horizontal streamlines are deflected laterally as
columns move up the slope and for sufficiently large y are again straight and
parallel to the vertical walls. Letting $q(x)$ denote the y component of velocity
far downstream, we see that

$$\frac{f}{H} = \frac{f+q'(x)}{H-M_0}, \tag{2.2a}$$

or
$$q'(x) = -fM_0/H. \tag{2.2b}$$

Integrating (2.2b) and evaluating the resulting constant by requiring the mass
flow rate to be identical upstream and downstream, we obtain

$$q(x) = \frac{VH}{H-M_0} - \frac{fM_0}{H}(x - \tfrac{1}{2}L), \tag{2.3}$$

where V represents the velocity far upstream. This represents a linear horizontal-
shear flow with a velocity which decreases to the right looking downstream.

This velocity will be somewhere negative and there will hence be blocking if

$$\tfrac{1}{2}fM_0\frac{L}{H} > VH/(H-M_0), \tag{2.4}$$

that is, if the Rossby number

$$R \equiv V/(fL) < M_0(H-M_0)/2H^2, \tag{2.5a,b}$$

or
$$M_0/H > \tfrac{1}{2}[1 - (1 - 8R)^{\frac{1}{2}}] \qquad (2.6a)$$

$$= 2R + 4R^2 + O(R^3) \quad (R \to 0). \qquad (2.6b)$$

The second solution of (2.5) has been discarded because it is the minimum critical condition, expressed by (2.6), which is sought.

The above theory needs to be modified for very small values of R because the Ekman suction velocities arising from the viscous boundary layers then produce significant effects that need to be added to the inertial effects considered above. For a discussion of the viscous regime the reader is referred to Huppert & Stern (1974).

A blocking effect that is qualitatively similar to that discussed above has been observed by Faller in an experiment cited by Phillips (1963). An obstacle of constant cross-section was placed along a radial arm in a tank filled with water and the system rotated at a constant angular velocity for a time sufficiently long for the water to be in a state of rigid-body rotation. A differential velocity between the obstacle and the fluid was then generated by an impulsive change in the rotation rate. As the fluid adjusted to the new rigid-rotation state, the Rossby number steadily decreased. Initially, at high Rossby numbers, the water flowed over the obstacle, while for smaller Rossby numbers the flow was more nearly parallel to the obstacle. Such a result is in qualitative agreement with the criterion (2.5).

3. The stratified, rotating equations and their solution

In this section we consider the flow in an infinitely deep channel, while the effects of finite depth are considered in §5. The vertical elevation of the rigid bottom is given by $z = M(x, y) = M_0 h(x/L) s(y/L)$, where $h(x/L)$ and $s(y/L)$ are non-dimensional functions of maximum value unity with either $s(\pm\infty) = 0$ or else $s(y/L)$ cyclic. As before, the channel is bounded by vertical walls at $x = 0, L$. A sketch of this system is presented in figure 2. The basic state, with $M(x, y) = 0$, consists of a velocity $(0, V, 0)$ and a density distribution $\rho_0 e^{-\beta z}$. The Brunt–Väisälä frequency is hence constant and given by

$$N = (g\beta)^{\frac{1}{2}}. \qquad (3.1)$$

The subsequent analysis is linearized and our aim is to determine the flow field resulting from the interaction of the variable bottom and the side walls in this rotating stratified system.

Denoting the perturbation velocity components by (u, v, w), the perturbation density by ρ and the perturbation pressure by p, we write the steady, linearized, Boussinesq equations of motion as

$$Vu_y - fv = -\rho_0^{-1} p_x, \quad Vv_y + fu = -\rho_0^{-1} p_y, \qquad (3.2), (3.3)$$

$$0 = g\rho + p_z, \qquad (3.4)$$

$$V\rho_y - \beta\rho_0 w = 0 \qquad (3.5)$$
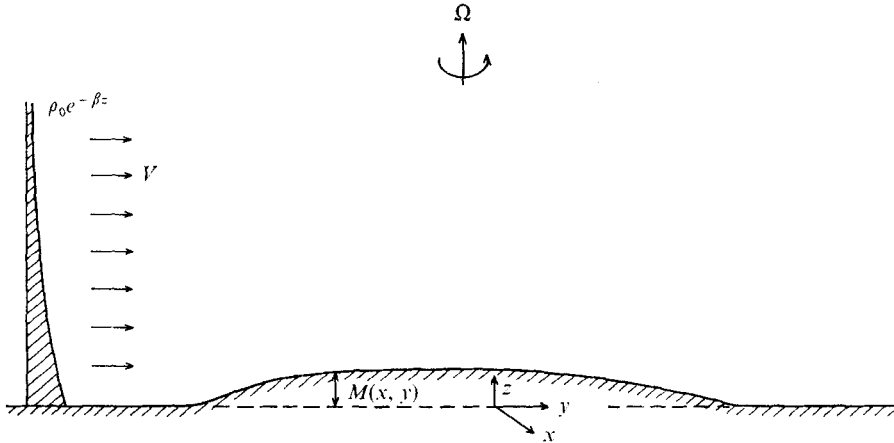
and
$$u_x + v_y + w_z = 0. \qquad (3.6)$$

FIGURE 2. An elevation of the channel of semi-infinite depth considered
in §§3 and 4.

In writing down the above, we have assumed the motion to be non-diffusive and hydrostatic $[V^2/(N^2L^2) \ll 1]$ and we have used an f-plane approximation.†

Eliminating v from (3.2) and (3.3), we obtain

$$\mathscr{L}u = -\rho_0^{-1}(V\partial_{xy}+f\partial_y)p, \qquad (3.7)$$

where

$$\mathscr{L} \equiv V^2\partial_{yy}+f^2. \qquad (3.8)$$

Similarly, eliminating u, we obtain

$$\mathscr{L}v = -\rho_0^{-1}(V\partial_{yy}-f\partial_x)p. \qquad (3.9)$$

Eliminating ρ from (3.4) and (3.5), we obtain

$$w = -(V/N^2\rho_0)p_{yz}. \qquad (3.10)$$

Equations (3.7), (3.9) and (3.10) can now be substituted into (3.6) to yield the equation for p:

$$V\partial_y\left(\partial_{xx}+\partial_{yy}+\frac{f^2}{N^2}\partial_{zz}+\frac{V^2}{N^2}\partial_{yyzz}\right)p = 0. \qquad (3.11)$$

This equation has a first integral

$$\left(\partial_{xx}+\partial_{yy}+\frac{f^2}{N^2}\partial_{zz}+\frac{V^2}{N^2}\partial_{yyzz}\right)p = 0, \qquad (3.12)$$

where the arbitrary function of integration has been set equal to zero because either p and its derivatives vanish as $y \to \infty$, or p is cyclic.

The boundary condition of zero normal velocity at $x = 0, L$ is obtained from (3.7), which upon integration states that

$$fp + Vp_x = 0 \quad (x = 0, L). \qquad (3.13\,a,b)$$

† By f-plane approximation we mean here that: the z axis is perpendicular to the undisturbed, parabolic isopycnals; the vertical component of the Coriolis force is neglected in the momentum equations; and a Cartesian representation is used.

The linearized boundary condition at $z = 0$ is obtained from $w = VM_y$ with w given by (3.10); hence

$$p_z = -\rho_0 M_0 N^2 h(x/L)\, s(y/L) \quad (z = 0). \tag{3.14}$$

For the vertically bounded model we require that

$$p < \infty \quad (z \to \infty) \tag{3.15}$$

plus a radiation condition which specifies that the perturbation consists only of waves propagating upwards. For a vertically bounded channel the radiation condition is unnecessary and (3.15) is replaced by the boundary condition $w = 0$ on the upper lid.

The system, say S, consisting of the differential equation (3.12), the boundary conditions (3.13)–(3.15) and the radiation condition is most conveniently investigated by expressing $s(y/L)$ in terms of its Fourier transform $\hat{s}(k)$,

$$s(y/L) = 2\mathscr{R}\left\{\int_0^\infty \hat{s}(k)\, e^{-iky}\, dk\right\} \tag{3.16a}$$

$$= \int_{-\infty}^\infty \hat{s}(k)\, e^{-iky}\, dk, \tag{3.16b}$$

(where $\mathscr{R}$ implies 'the real part of') and solving for each downstream wavelength independently. Introducing the non-dimensional variables ξ, ζ and ϕ by the transformations,

$$x = L\xi, \quad z = (fL/N)\zeta \tag{3.17},(3.18)$$

and

$$p = 2\rho_0 M_0 fLN\mathscr{R}\left\{\int_0^\infty \hat{s}(k)\, \phi(\xi,\zeta;k)\, e^{-iky}\, dk\right\} \tag{3.19a}$$

$$= \rho_0 M_0 fLN \int_{-\infty}^\infty \hat{s}(k)\, \phi(\xi,\zeta;k)\, e^{-iky}\, dk, \tag{3.19b}$$

we substitute (3.16)–(3.19) into S to obtain the system, say S',

$$\phi_{\xi\xi} + \phi_{\zeta\zeta} - k^2 L^2(\phi + R^2\phi_{\zeta\zeta}) = 0, \tag{3.20}$$

$$\phi + R\phi_\xi = 0 \quad (\xi = 0, 1), \tag{3.21a,b}$$

$$\phi_\zeta = -h(\xi) \quad (\zeta = 0), \tag{3.22}$$

$$\phi < \infty \quad (\zeta \to \infty) \tag{3.23}$$

plus a suitable radiation condition, where $R = V/(fL)$. In S' the dependent variable ϕ is $(\rho_0 fLN)^{-1}$ times the perturbation pressure resulting from the flow over the bottom topography

$$M_0 h(x/L)\, e^{-iky}. \tag{3.24}$$

While in appendix A we present the exact solution of S', the major features of the solution can be obtained from a long-wavelength approximation. Thus, we let $k \to 0$ in S' to obtain the system S_0',

$$\phi_{\xi\xi} + \phi_{\zeta\zeta} = 0, \tag{3.25}$$

$$\phi + R\phi_\xi = 0 \quad (\xi = 0, 1), \tag{3.26a,b}$$

$$\phi_\zeta = -h(\xi) \quad (\zeta = 0), \tag{3.27}$$

$$\phi < \infty \quad (\zeta \to \infty), \tag{3.28}$$

plus a suitable radiation condition. These equations describe the flow field in the limit

$$kL \to 0 \quad R \lesssim O(1). \qquad (3.29\,a,b)$$

In an entirely quasi-geostrophic analysis the governing differential equation is still (3.25), but the corresponding boundary condition at $\xi = 0, 1$ degenerates to $\phi = 0$. Thus the system S_0' describes the ageostrophic response since the Rossby number is included in the side-wall boundary condition (3.26). We remark that the long-wavelength limit (3.29) can be formally obtained by neglecting the first term in (3.2), that is by specifying the flow to be strictly geostrophic in the cross-stream direction, but not necessarily in the downstream direction. These long-wave equations filter out the inertia–gravity waves but not the Kelvin waves.

For non-zero values of R, the solution of (3.25) and (3.26) can be written as

$$\phi = \sum_{n=1}^{\infty} (A_n/n\pi)\,\chi_n(\xi)\,e^{-n\pi\zeta} - RB\theta(\xi)\,[\sin(\zeta/R) + C\cos(\zeta/R)], \qquad (3.30)$$

where

$$\chi_n(\xi) = \sin n\pi\xi - n\pi R \cos n\pi\xi \qquad (3.31)$$

and

$$\theta(\xi) = e^{-\xi/R}. \qquad (3.32)$$

The functions $\chi_n(\xi)$ and $\theta(\xi)$ are the eigenfunctions of the ordinary Sturmian system

$$y''(\xi) - \lambda^2 y(\xi) = 0, \qquad (3.33)$$

$$y(\xi) + Ry'(\xi) = 0 \quad (\xi = 0, 1), \qquad (3.34\,a,b)$$

and thus form a complete orthogonal set on $[0, 1]$ with inner products

$$\langle \chi_n, \chi_m \rangle = \langle \chi_n, \theta \rangle = 0 \quad (n \neq m), \qquad (3.35\,a,b)$$

$$\langle \chi_n, \chi_n \rangle = \tfrac{1}{2}(1 + n^2\pi^2 R^2), \qquad (3.36)$$

and

$$\langle \theta, \theta \rangle = \tfrac{1}{2}R(1 - e^{-2/R}), \qquad (3.37)$$

where

$$\langle \Phi, \Psi \rangle \equiv \int_0^1 \Phi(\xi)\,\Psi(\xi)\,d\xi \qquad (3.38)$$

for arbitrary functions $\Phi(\xi)$ and $\Psi(\xi)$. Differentiating (3.30) with respect to ζ, setting $\zeta = 0$, substituting the result into (3.27) and using the orthogonality property of the χ_n and θ, we determine the A_n and B as

$$A_n = \langle h, \chi_n \rangle / \langle \chi_n, \chi_n \rangle, \qquad (3.39)$$

$$B = \langle h, \theta \rangle / \langle \theta, \theta \rangle. \qquad (3.40)$$

When (3.30) is substituted into (3.27) the term containing C drops out and hence C must be determined from other considerations.

The radiation condition, which determines the value of C, follows from either of two considerations. A disturbance of the form $\exp(i\zeta/R)$ corresponds to an upward flux of energy ($\overline{wp} > 0$) for $k > 0$, whereas $\exp(-i\zeta/R)$ corresponds to downward propagation of energy and must hence be neglected. Alternatively, in a co-ordinate system moving downstream with speed V, computation of the group velocity (as explained, for example, by Lighthill 1965) shows that for all k the wave propagating energy upward is obtained by setting

$$C = i\,\mathrm{sgn}\,k. \qquad (3.41)$$

The normalized pressure response can now be calculated from (3.30), (3.39) and (3.40) and the perturbation velocities computed therefrom. For example, for the simplest case, for which $h(\xi) \equiv 1$,

$$A_n = \begin{cases} (4/n\pi)(1 + n^2\pi^2R^2)^{-1} & (n \text{ odd}), & (3.42a) \\ 0 & (n \text{ even}), & (3.42b) \end{cases}$$

$$B = 2(1 + e^{-1/R}), \qquad (3.43)$$

and the amplitude of the downstream perturbation velocity at the base of the left-hand wall, $\xi = \zeta = 0$, is

$$M_0N\left(\sum_{n=1}^{\infty} A_n - iB\right) \sim -(2M_0N/\pi)\log R \quad (R \to 0). \qquad (3.44), (3.45)$$

We note immediately from (3.45) that for this case the downstream velocity becomes infinitely large as $R \to 0$. We discuss this divergence further in the next section.

To determine the response for an arbitrary bottom topography we combine the various contributions of different wavelengths according to (3.19) to obtain

$$P \equiv p/(\rho_0 M_0 fLN) \qquad (3.46a)$$

$$= s(\eta)\sum_{n=1}^{\infty} \{A_n/n\pi\} \chi_n(\xi) e^{-n\pi\zeta} - RB\theta(\xi)[s(\eta)\sin(\zeta/R) - \tilde{s}(\eta)\cos(\zeta/R)], \quad (3.46b)$$

where

$$\eta = y/L, \qquad (3.47)$$

$$\tilde{s}(\eta) = \frac{1}{\pi}\int_{-\infty}^{\infty} \frac{s(t)}{t - \eta}\,dt = -i\int_{-\infty}^{\infty} \tilde{s}(k)\,\mathrm{sgn}\,k\,e^{-iky}\,dk \qquad (3.48a,b)$$

is the Hilbert transform of $s(\eta)$ (see, for example, Erdélyi *et al.* 1954, chap. 15) and the bar through the integral sign in (3.48a) indicates that only the principal part of the integral is to be considered.

For $R \equiv 0$ the normalized pressure response P is given by

$$P = 2s(\eta)\sum_{n-1}^{\infty} (n\pi)^{-1} < h, \sin n\pi\xi > \sin n\pi\xi\, e^{-n\pi\zeta}. \qquad (3.49)$$

4. Interpretation and discussion

The solution (3.46) is a combination of two parts. The first, expressed by the infinite sum, represents a geostrophic response modified by ageostrophic effects, which decays with height according to

$$\exp(-\pi\zeta) \quad \text{or} \quad \exp(-\pi Nz/fL), \qquad (4.1a,b)$$

and is hence trapped to within a dimensional height $fL/(\pi N)$ from the bottom. Since the streamlines have virtually no vertical deflexion above $fL/(\pi N)$, the reader will see that this trapping height plays a role which is qualitatively similar to that played by the lid in the homogeneous flow considered in §2. There is a vertical concentration of the streamlines as the stratified fluid flows over a rise, thereby inducing anticyclonic shear.

In order to explain the appearance of the last two terms in (3.46b) we remark that in an otherwise quiescent fluid there are oppositely propagating free internal Kelvin waves attached to both walls. When an obstacle is moved through such a fluid it excites only that Kelvin wave whose phase velocity equals the velocity of the obstacle. Thus, in the frame of reference used here a Kelvin wave appears only on the left-hand wall. This Kelvin wave has zero cross-stream velocity everywhere and is trapped to within a distance $V/f = RL$ from the wall. The wave propagates to an infinite height with a vertical wavelength given by $2\pi V/N = 2\pi(f/N)\,RL$ in dimensional units or $2\pi R$ in non-dimensional units. It should be noted that for small Rossby numbers the vertical wavelength of the Kelvin wave is very much less than the trapping height.

The vertically propagating internal Kelvin wave gives rise to a wave drag on the obstacle as a consequence of the vertical transport of momentum. We also point out that owing to the coupling of the quasi-geostrophic and Kelvin components a lateral Reynolds stress occurs. This stress can be evaluated by calculating the average of uv over one downstream wavelength, using the relationships for A_n and B given previously. These stresses will be important in modifying the basic current and should be taken into account in a finite amplitude study.

The relationship between the perturbation pressure and the downstream perturbation velocity is given by (3.9), which in the long-wave limit (3.29) reduces to

$$v = p_x/(\rho_0 f). \tag{4.2}$$

Using (3.46), we can thus write

$$v/(M_0 N) = s(\eta) \sum_{n=1}^{\infty} A_n \psi_n(\xi)\, e^{-n\pi\zeta} - B\theta(\xi)\,[s(\eta)\sin(\zeta/R) - \tilde{s}(\eta)\cos(\zeta/R)], \tag{4.3}$$

where

$$\psi_n(\xi) = \chi_n'(\xi)/(n\pi) = \cos n\pi\xi + n\pi R \sin n\pi\xi. \tag{4.4a,b}$$

An indication of the magnitude of the downstream perturbation velocity can be obtained by examining the convergence of the infinite sum in (4.3). We show rigorously in appendix B that as $R \to 0$ the infinite sum diverges, thus indicating that the downstream velocity is infinite, at the base of the wall $\xi = 0$, 1, $\zeta = 0$, unless $h(\xi) \to 0$ as $\xi \to 0$, 1. The explanation of this result is as follows. The vanishing of the cross-stream velocity at the side walls $\xi = 0, 1$ implies, using the downstream momentum equation (3.3) and assuming that v remains bounded as $R \to 0$, that $P = 0$ at $\xi = 0$, 1 for all ζ. From (3.14) we see that P_ζ at $\xi = 0$, 1 and $\zeta = 0$ is proportional to $h(\xi)$ at $\xi = 0, 1$. Thus, unless $h(\xi) \to 0$ as $\xi \to 0$, 1, there is a contradiction between the statements $P = 0$ for all ζ and $P_\zeta \neq 0$ at $\zeta = 0$. The implication of this contradiction is that the assumption that v remains bounded as $R \to 0$ is not valid.

Turning now to the Kelvin-wave contribution to v, we see from (4.3) that this is maximum at $\xi = 0$ and is of amplitude

$$M_0 N B[s^2(\eta) + \tilde{s}^2(\eta)]^{\frac{1}{2}}. \tag{4.5}$$

Using (3.40) to evaluate B for small R, we calculate that

$$B \sim 2[h(0) + Rh'(0) + O(R^2)] \quad (R \to 0). \tag{4.6}$$

Thus the Kelvin wave, which is absent at strictly zero Rossby number, makes a contribution to the horizontal velocity which does not tend to zero as the Rossby number tends to zero if $h(0) \neq 0$. This is also true of the vertical velocity. Such a discontinuous situation is a familiar consequence of singular perturbation problems, indicated in this case by the small parameter R multiplying the highest derivative in the boundary condition (3.21).

When the perturbation velocity becomes equal and opposite to the free-stream velocity blocking will occur. Although the investigation of such a phenomenon requires a careful consideration of nonlinear effects, we can estimate the critical point at which blocking occurs and also conveniently summarize the results of our linear theory as follows. We calculate, for given R, the maximum negative value of v from (4.3), and equating this to $-V$ determine the maximum value of an inverse Froude number

$$(M_0 N / V)_{\max} = \kappa, \tag{4.7}$$

say, for which the present, linearized analysis predicts a flow without a stagnation region. Since v is a solution of the two-dimensional Laplacian in (ξ, ζ) variables, it attains its extrema on the boundaries (either side or bottom) of the channel. We use this fact in the following investigation of two particular examples. In the first example, we consider the cross-stream profile to be given by $h(\xi) = 1$ and in the second by $h(\xi) = \sin \pi \xi$. For both examples we take the downstream profile to be the Witch of Agnesi $s(\eta) = (1 + \eta^2)^{-1}$, for which

$$\tilde{s}(\eta) = -\eta (1 + \eta^2)^{-1},$$

although the results should be representative for any $s(\eta)$ which is an even function of η and which with its first derivative is continuous in $-\infty < \eta < \infty$.

Example (i) $h(\xi) s(\eta) = (1 + \eta^2)^{-1}$.

Applying to this profile the general considerations discussed above, we conclude that for $R = 0$, v is minus infinity at $\xi = 1$. Thus κ approaches zero as $R \to 0$. Substituting (3.42) and (3.43) into (4.3) we find that for sufficiently small R the maximum negative value of v occurs at $(\xi, \eta, \zeta) = (1, \eta_1, 0)$, where

$$\eta_1 = \left\{ \left[\left(\sum_{n=1}^{\infty} A_n \right)^2 + B^2 e^{-2/R} \right]^{\frac{1}{2}} - \sum_{n=1}^{\infty} A_n \right\} B^{-1} e^{1/R} \tag{4.8a}$$

$$\sim \tfrac{1}{2}\pi \, e^{-1/R} (\log R)^{-1} \quad (R \to 0) \tag{4.8b}$$

and
$$\sum_{n=1}^{\infty} A_n = \frac{2}{\pi} \mathscr{R} \left\{ 2\psi \left(\frac{i}{\pi R} \right) - \psi \left(\frac{i}{2\pi R} \right) + \gamma \right\} \tag{4.9a}$$

$$= \frac{2}{\pi} \left[\log \frac{2}{\pi R} + \gamma - \tfrac{1}{6}\pi^2 R^2 + O(R^4) \right]. \tag{4.9b}$$

In (4.9), $\psi(z)$ is the digamma function (Abramowitz & Stegun 1964, p. 258) and $\gamma = 0.577\ldots$ is Euler's constant. Evaluating (4.3) at $(1, \eta_1, 0)$, we determine that

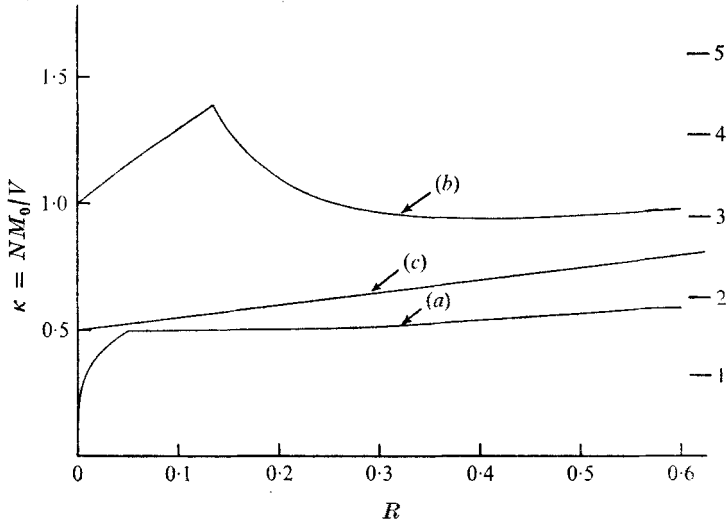$$v(1, \eta_1, 0) = -\tfrac{1}{2} M_0 N B \, e^{-1/R} \eta_1^{-1} \tag{4.10}$$

FIGURE 3. The parameter $\kappa = NM_0/V$ at stagnation versus the Rossby number. (a) $M(\xi, \eta) = M_0/(1+\eta^2)$, $0 \leqslant \xi \leqslant 1$. The critical condition is caused by the modified quasi-geostrophic component for $R < 0.048$ and by the Kelvin wave for $R > 0.048$. (b) $M(\xi, (\sin \pi\xi)/(1+\eta^2)$, $0 \leqslant \xi \leqslant 1$. The critical condition is caused by the modified quasi-geostrophic component for $R < 0.135$ and by the Kelvin wave for $R > 0.135$. (c) $M(\xi, \eta) = M_0 e^{-\xi}/(1+\eta^2)$, $0 \leqslant \xi < \infty$. The critical condition is caused by the Kelvin wave for all R. The marks with their corresponding number m at the right edge of the figure indicate the resonance position of the first m modes for a bounded channel of maximum bottom elevation to depth ratio M_0/H equal to 0.1.

and hence that
$$\kappa = 2\eta_1 B^{-1} e^{1/R} \qquad (4.11a)$$

$$= \left(\sum_{n=1}^{\infty} A_n \right)^{-1} [1 + O(e^{-2/R})] \quad (R \to 0). \qquad (4.11b)$$

This critical value of $M_0 N/V$ is correct, however, only for $0 < R < 0.048$, wherein $0 > \eta_1 > -0.9 \times 10^{-9}$. For $R > 0.048$ the maximum negative value of v is due entirely to the Kelvin wave. This maximum value, which occurs at $(0, 0, \zeta_n)$, where

$$\zeta_n = (2n - \tfrac{1}{2}) \pi R$$

for positive integer values of n sufficiently large that the first term in (4.3) may be neglected, is given by
$$v(0, 0, \zeta_n) = -M_0 NB. \qquad (4.12)$$

Hence
$$\kappa = B^{-1} \quad (R > 0.048). \qquad (4.13)$$

These results are presented graphically in figure 3.

Example (ii) $h(\xi) s(\eta) = \sin(\pi\xi)(1+\eta^2)^{-1}$

In contrast to the preceding example, the bottom variation considered here includes a cross-stream variation and the fluid can hence flow around as well as over the bottom contours. Further, the height of the topography is zero at the

channel walls and hence the velocities are bounded for all values of the Rossby number. To evaluate κ, we proceed as before and determine that

$$A_1 = (1 + \pi^2 R^2)^{-1}, \tag{4.14a}$$

$$A_n = \begin{cases} 4\pi R[(1 + n^2\pi^2 R^2)(n^2 - 1)]^{-1} & (n \text{ even}), & (4.14b) \\ 0 & (n \text{ odd}, n \neq 1) & (4.14c) \end{cases}$$

and that
$$B = -2\pi R[(1 + \pi^2 R^2)(1 - e^{1/R})]^{-1}. \tag{4.15}$$

Numerical calculation shows that for $R < 0.135$ the maximum negative value of v occurs at $\zeta = 0$, $\eta = \eta_2 \simeq 0$ and a value of ξ which decreases monotonically from 1 at $R = 0$ to 0.914 at $R = 0.135$. The resulting value of κ is presented in figure 3. For $R > 0.135$ the stagnation point again first occurs at $(0, 0, \zeta_n)$, where the negative horizontal velocity of the Kelvin wave is a maximum.

We see that, for both these examples, for sufficiently small values of the Rossby number the analysis predicts a stagnation point first appearing on the bottom of the channel on (example i) or near (example ii) the right-hand wall looking downstream, while for larger values of the Rossby number the stagnation point occurs high up on the left-hand wall.

5. Flow in a channel with a lid

We now consider the flow in a channel with a rigid horizontal lid at a height $z = H$. The radiation condition which applies to the unbounded channel is replaced by the boundary condition $w(x, y, H, t) = 0$, which with (3.10) implies that $p_z(x, y, H, t) = 0$. Thus the system to be considered is

$$\phi_{\xi\xi} + \phi_{\zeta\zeta} = 0, \tag{5.1}$$

$$\phi + R\phi_\xi = 0 \quad (\xi = 0, 1), \tag{5.2a, b}$$

$$\phi_\zeta = -h(\xi) \quad (\zeta = 0), \tag{5.3}$$

$$\phi_\zeta = 0 \quad (\zeta = \zeta_0), \tag{5.4}$$

where
$$\zeta_0 = NH/(fL). \tag{5.5}$$

Using the methods described in §3, we determine the solution of (5.1)–(5.4) for ϕ and then carry out the Fourier transform (3.19) to obtain, after use of (3.46a),

$$P(\xi, \eta, \zeta) = s(\eta)\left\{ \sum_{n=1}^{\infty} \frac{A_n \chi_n(\xi) \cosh n\pi(\zeta_0 - \zeta)}{n\pi \sinh n\pi\zeta_0} - \frac{RB\theta(\xi)}{\sin \zeta_0/R} \cos\left(\frac{\zeta_0 - \zeta}{R}\right) \right\}, \tag{5.6}$$

where the A_n and B are given by (3.39) and (3.40). We notice that allowing for both upward- and downward-propagating waves over a slowly varying bottom (3.29) yields a response which at any downstream point, say η_0, is proportional simply to $s(\eta_0)$ [and $\tilde{s}(\eta_0)$, for example, is not relevant].

The essential features of the solution (5.6) are the same as those previously considered, in particular the existence of a trapped Kelvin wave which has a singular behaviour as the Rossby number tends to zero. The only new feature added is the possibility of a resonance if $\sin(\zeta_0/R) = 0$, that is if

$$\zeta_0/R = n\pi \quad (n = 1, 2, \ldots) \tag{5.7}$$

or, in dimensional terms,
$$NH/V = n\pi, \tag{5.8}$$

in which case a Kelvin wave of undetermined amplitude may be added to any solution. We have marked the first five resonance points on figure 3 for a ratio M_0/H, of maximum obstacle height to channel height, of 0·1. This form of resonance is a familiar result of linearized analysis applied to flows with lids and has been extensively considered for stratified flows without rotation by Miles (1968) and Davis (1969) amongst others.

6. Flow in a channel with only one wall

Since the Kelvin wave is trapped near the left-hand wall, we would anticipate that it and the subsequent flow are not significantly affected by removing the wall at $x = L$. The flow in the channel of semi-infinite width is described by

$$\phi_{\xi\xi} + \phi_{\zeta\zeta} = 0, \tag{6.1}$$

$$\phi + R\phi_\xi = 0 \quad (\xi = 0), \tag{6.2}$$

$$\phi_\zeta = -h(\xi) \quad (\zeta = 0), \tag{6.3}$$

$$\phi < \infty \quad (\zeta \to \infty) \tag{6.4}$$

plus an appropriate radiation condition. There is no solution of (6.1)–(6.4) unless $h(\xi) \to 0$ as $\xi \to \infty$ [equation (6.6)], in particular there is no solution for $h(\xi) \equiv 1$.

Generalizing the approach of §3, we determine the following expression for P, which results from the solution of (6.1)–(6.4):

$$P(\xi, \eta, \zeta) = s(\eta) \int_0^\infty \alpha(\lambda) \left(\sin \lambda\xi - R\lambda \cos \lambda\xi\right) e^{-\lambda\zeta} d\lambda + R\beta\theta(\xi) \left[s(\eta) \sin (\zeta/R)\right.$$
$$\left. - \tilde{s}(\eta) \cos (\zeta/R)\right], \tag{6.5}$$

where

$$\alpha(\lambda) = \frac{2}{\pi\lambda(1 + R^2\lambda^2)} \int_0^\infty (\sin \lambda\xi - R\lambda \cos \lambda\xi) h(\xi) \, d\xi \tag{6.6}$$

and

$$\beta = -2R^{-1} \int_0^\infty h(\xi) e^{-\xi/R} \, d\xi. \tag{6.7}$$

For $R = 0$, the second term in the integrals in (6.5) and (6.6), together with the last two terms in (6.5) are omitted from the solution. As before, the first term in (6.5) represents a modified geostrophic flow which is trapped near the bottom, while the second and third term together describe an internal Kelvin wave of positive vertical group velocity.

An examination of the finiteness of the flow (6.5) involves determining the magnitude of $\alpha(\lambda)$ for large positive λ. Using well-known results in conjunction with (6.5*a*) (Lighthill 1962, example 34) we obtain

$$\alpha(\lambda) \sim \begin{cases} 2(\pi R^2\lambda^4)^{-1} [h(0) + Rh'(0)] + O(\lambda^{-6}) & (R \neq 0), & (6.8) \\ 2(\pi\lambda^2)^{-1} h(0) + O(\lambda^{-4}) & (R = 0). & (6.9) \end{cases}$$

Hence the velocities derived from (6.5) are finite for all non-zero R, but the downstream and vertical velocities will be infinite for $R = 0$ at $\xi = \zeta = 0$ unless $h(\xi) \to 0$ as $\xi \to 0$. Further, writing (6.5*b*) for small R as

$$\beta \sim -2h(0) - 2Rh'(0) + O(R^2), \tag{6.10}$$

we determine that, in analogy with §4, only if $h(\xi) \to 0$ as $\xi \to 0$ does the horizontal velocity in the Kelvin wave approach zero as the Rossby number approaches zero.

The value of κ may be determined in a manner similar to that described above. In particular, if $h(\xi) s(\eta) = e^{-\xi}(1+\eta^2)^{-1}$, we find that

$$\alpha(\lambda) = 2(1-R)[\pi(1+R^2\lambda^2)(1+\lambda^2)]^{-1}, \tag{6.11}$$

$$\beta = -2(1+R)^{-1} \tag{6.12}$$

and that the maximum negative value of v is that due solely to the Kelvin wave for all values of R, occurring at $(0, 0, \zeta_n)$ with a resulting value of $\frac{1}{2}(1+R)$ for κ.

We have discussed the flow in a channel with a left-hand wall only and shown that the flow field is a combination of a modified quasi-geostrophic component and an internal Kelvin wave. In contrast, the flow in a channel with a right-hand wall only will consist solely of a modified quasi-geostrophic component since a steady internal Kelvin wave cannot exist trapped near a right-hand wall. The explicit solution can be obtained by the methods outlined above, but is of minor interest and will not be discussed further.

7. Conclusions

When a homogeneous fluid flows over a rise in a vertically bounded, rotating channel (figure 1) it develops negative relative vorticity and is deflected to the left in the manner described in §2. If the fluid is stratified, the flow consists of a combination of a modified quasi-geostrophic flow trapped near the bottom and a strictly ageostrophic, internal Kelvin wave trapped near the left-hand wall. The modified quasi-geostrophic flow is qualitatively similar to the homogeneous flow mentioned previously, with an effective vertical depth supplied by the trapping length fL/N.

For a channel with two vertical walls and a bottom elevation which varies in the downstream direction only, if $0 < R < 0.048$ the minimum downstream velocity is due to the modified quasi-geostrophic component and occurs at the base of the right-hand wall. Determining the stagnation condition by extrapolation, we find that the critical bottom elevation is given by

$$M_0/L \sim -(f/N)R\log R \quad (R \to 0).$$

If $R > 0.048$ the minimum downstream velocity occurs at the minima of the Kelvin-wave contribution and the critical bottom elevation is given by

$$M_0/L = \tfrac{1}{2}(f/N)R(1+e^{-1/R}) \quad (R > 0.048).$$

Qualitatively similar results are valid for more general bottom elevations, as shown for a particular example in figure 3.

For a channel with only a left-hand wall the minimum downstream velocity occurs on that wall at the minima of the Kelvin wave for all Rossby numbers.

Appendix A

In this appendix we examine briefly the consequence of relaxing the approximations (3.29) considered through the rest of the paper. This will introduce the additional effects of inertia–gravity waves. However, the resulting flow can be discussed in ways very similar to those already presented. Only the flow in a channel with two vertical walls and of infinite height will be considered and we thus seek the solution of the system S'. This can be obtained by the methods outlined above to yield

$$\phi(\xi, \zeta; k) = \left\{ \sum_{n=1}^{\infty} \frac{\hat{C}_n(k)}{n\pi} \chi_n(\xi) \exp\left[-\left(\frac{n^2\pi^2 + k^2 L^2}{1 - R^2 k^2 L^2} \right)^{\frac{1}{2}} \right] \right\}$$
$$- RB\theta(\xi) \left[\sin(\zeta/R) + i \operatorname{sgn} k \cos(\zeta/R) \right], \quad \text{(A1)}$$

where
$$\hat{C}_n(k) = \frac{2n\pi}{1 + n^2\pi^2 R^2} \left(\frac{1 - R^2 k^2 L^2}{n^2\pi^2 + k^2 L^2} \right)^{\frac{1}{2}} \langle \chi_n, h \rangle \quad \text{(A2)}$$

and
$$\left(\frac{n^2\pi^2 + k^2 L^2}{1 - R^2 k^2 L^2} \right)^{\frac{1}{2}} = i \left| \frac{n^2\pi^2 + k^2 L^2}{1 - R^2 k^2 L^2} \right| \operatorname{sgn} k \quad (|kL| > R^{-1}). \quad \text{(A3)}$$

The inertia–gravity waves are represented in (A1) by the contribution to the Fourier transform (3.19) for $|kL| > R^{-1}$ and the determination of the sign of the radical in (A1) by (A3) is a consequence of the radiation condition. We note that these inertia–gravity waves do not contribute to the solution (3.19) if $s(k)$ has support only within $-R^{-1} < kL < R^{-1}$, that is if there are no variations in $\zeta(\eta)$ on length scales less than R.

Appendix B

In this appendix we examine the convergence of the infinite sum in (4.3). This convergence is dependent upon the size of A_n for large n. Using (3.39), we can write

$$A_n = -2(1 + n^2\pi^2 R^2)^{-1} \int_0^1 \cos(n\pi\xi + \epsilon_n) h(\xi) \, d\xi, \quad \text{(B1)}$$

where
$$\tan \epsilon_n = (n\pi R)^{-1} \quad (0 \leqslant \epsilon_n < \tfrac{1}{2}\pi). \quad \text{(B2)}$$

Expanding the integrand in (B1) for large n, we obtain

$$A_n \sim -2(n\pi R)^{-1} \mathscr{R} \left\{ [1 + i(n\pi R^{-1})] \int_0^1 h(\xi) e^{-in\pi\xi} \, d\xi \right\} [1 + O(n^{-1})], \quad \text{(B3)}$$

valid for fixed, non-zero R.

The asymptotic form of the integral in (B3) can now be evaluated by standard techniques (see, for example, Lighthill 1962, §5.5). In particular, if the bottom topography smoothly spans the channel, that is both $h(\xi)$ and $h'(\xi)$ are continuous in $[0, 1]$, then

$$A_n \sim -2R^{-1}(n\pi)^{-3} \{(-1)^n h'(1) - h'(0) + R^{-1}[(-1)^n h(1) - h(0)]\} + O(n^{-4}), \quad \text{(B4)}$$

from which we conclude that the infinite sum in (4.3) is pointwise convergent and bounded. This is not necessarily true if $R = 0$, for which

$$A_n = 2\int_0^1 h(\xi) \sin n\pi\xi \, d\xi \tag{B 5}$$

$$\sim -2(n\pi)^{-1}[(-1)^n h(1) - h(0)] + O(n^{-3}). \tag{B 6}$$

The downstream velocity is then plus (minus) infinity at the bottom of the channel wall, $\xi = 0$ (1) and $\zeta = 0$, unless $h(\xi) \to 0$ as $\xi \to 0$ (1). Thus the quasi-geostrophic calculation leads to an unacceptable, infinite downstream velocity if the bottom topography does not go to zero at the walls. The conclusions of this paragraph also hold for the vertical velocity, but not for the cross-stream velocity, which is always finite.

Alternatively, if the bottom topography does not completely span the channel, with $h(\xi)$ and $h'(\xi)$ continuous only in the range say $[\xi_1, \xi_2]$ and zero elsewhere, then a similar analysis to that of the preceding paragraph proves that the velocity for all values of R is bounded except at the end of the obstacle $\xi = \xi_1(\xi_2)$ and $\zeta = 0$, unless $h(\xi) \to 0$ as $\xi \to \xi_1 (\xi_2)$. That is, the linearized analysis is capable of handling most isolated obstacles, but not those with vertical walls, as would occur, for example, in a 'top-hat' cross-section.

REFERENCES

ABRAMOWITZ, M. & STEGUN, I. A. 1964 *Handbook of Mathematical Functions.* U.S. Government Printing Office.

DAVIS, R. E. 1969 The two-dimensional flow of a stratified fluid over an obstacle. *J. Fluid Mech.* **36**, 127–143.

ERDÉLYI, A., MAGNUS, W., OBERHETTINGER, F. & TRICOMI, F. G. 1954 *Tables of Integral Transforms*, vol. 2. McGraw-Hill.

HOGG, N. 1973 On the stratified Taylor column. *J. Fluid Mech.* **58**, 517–537.

HUPPERT, H. E. 1974 Some remarks on the initiation of inertial Taylor columns. *J. Fluid Mech. (subjudice).*

HUPPERT, H. E. & STERN, M. E. 1974 The effect of side walls on homogeneous, rotating flow over two-dimensional obstacles. *J. Fluid Mech.* **62**, 417–436.

LIGHTHILL, M. J. 1962 *An Introduction to Fourier Analysis and Generalised Functions.* Cambridge University Press.

LIGHTHILL, M. J. 1965 Group velocity. *J. Inst. Maths. Applics.* **1**, 1–28.

MILES, J. W. 1968 Lee waves in a stratified flow. Part 1. Thin barrier. *J. Fluid Mech.* **32**, 549–567.

MILES, J. W. 1969 Waves and wave drag in stratified flows. *Proc. 12th Int. Congr. Appl. Mech., Stanford University.*

PARKER, C. E. 1971 Gulf Stream rings in the Sargasso Sea. *Deep-Sea Res.* **18**, 981–993.

PHILLIPS, N. A. 1963 Geostrophic motion. *Rev. Geophys.* **1**, 123–176.

RICHARDSON, P. L., STRONG, A. E., & KNAUSS, J. A. 1973 Gulf Stream eddies: Recent observations in the Western Sargasso Sea. *J. Phys. Oceanog.* **3**, 297–301.

WEBSTER, F. 1968 Observations of inertial-period motions in the deep sea. *Rev. Geophys.* **6**, 473–490.